SUPPLEMENT TO THE WELDING JOURNAL, FEBRUARY 2006
Sponsored by the American Welding Society and the Welding Research Council

Ranking the Resistance of Wrought Superalloys to Strain-Age Cracking

The controlled heat rate test was used to rank the crack resistance of several alloys, and a correlation between alloy performance and chemical composition was established

BY M. D. ROWE

ABSTRACT. High-strength, heat-resistant alloys are critical construction materials for modern gas turbines used in power generation and aviation applications. The use of higher-strength alloys has long been limited by the susceptibility of some of these alloys to strain-age cracking during postweld heat treatment. No widely accepted test method exists that provides an easy and economical method of ranking the resistance of alloys to strain-age cracking. Of the test methods that appear in the literature, the controlled heating rate test (CHRT), developed in the 1960s, stands out because it is simple and economical as well as having been correlated to restrained weldment test results. In this investigation, the CHRT was used to rank several commercial alloys by their resistance to strain-age cracking, and alloy performance was correlated to chemical composition.

Introduction

Strain-age cracking is a problem that can occur during post-fabrication heat treatment of alloys that strengthen by precipitation of γ'. Typically, these are nickel-based alloys that contain aluminum and/or titanium, either for high-temperature strength or oxidation resistance. Cracking can occur when an alloy that contains γ'-forming elements in solid solution is heated through a temperature range in which γ' precipitates, about 1100° to 1800°F (590° to 980°C), during the postweld solution annealing heat treatment. During the precipitation of γ', the ductility of the alloy may drop to a very low level, and cracking can occur if the alloy is subjected to a level of strain that exceeds the available ductility. In a restrained fabrication, tensile stress develops as a result of the volume contraction that is associated with the formation of γ' from solid solution. The problem is aggravated by a coarse grain size, the presence of an oxidizing atmosphere, and constitutional liquation of carbides, which can further degrade ductility (Ref. 1). Cracking is frequently associated with weldments because of residual stress, grain growth, constitutional liquation in the heat-affected zone (HAZ), and the stress concentration at the toe of the weld. However, cracking can occur in the unaffected base metal in addition to the weld metal and HAZ.

A test method that is capable of ranking the resistance of alloys to strain-age cracking is needed in the development of new alloys. In order to accomplish the alloy-development objective, it is necessary to compare the weldability of newly developed experimental alloys to each other and to existing commercial alloys. In order to be effective, the test method must produce a quantitative index of weldability, require a minimum of material and labor, and be possible to implement with readily available and inexpensive equipment.

Review of Strain-Age Cracking Test Methods

Early investigators used the restrained circular patch test to evaluate the resistance of alloys to strain-age cracking (Refs. 2, 3). The circular patch test has the advantage of employing an actual restrained weldment, which is similar to a real fabrication. However, the test is only reproducible if the parts are precisely machined and joined with a highly controlled, automated welding process (Ref. 4). The restrained weldment test is useful to demonstrate that an alloy can be welded, but has many disadvantages as a ranking test. The test requires a large investment of labor and material, many variables are involved that are difficult to control, the result is semiquantitative at best, and the level of restraint cannot be varied easily. Some investigators reported that the level of restraint in a circular patch test is only sufficient to crack R-41 alloy in a repair-weld simulation, but not in the original weld (Refs. 2, 3). A test that cannot crack a susceptible alloy such as R-41 in a reproducible manner is not useful in ranking more-resistant alloys.

Several investigators have used the Gleeble thermomechanical testing apparatus to simulate strain-age cracking (Refs. 5–11). The Gleeble offers broad flexibility in the thermal cycles and mechanical strain that can be applied, which has led to a wide variety of test methods and specimen geometries. Many of the Gleeble tests use a round-bar specimen, which is not suitable for testing sheet material. A Gleeble test for use on sheet material was developed by Nakao (Ref. 9). This method uses a notched sheet specimen, and allows for determining the effect of a wide variety of welding or heat treatment thermal cycles on the ductility of various alloys. The various Gleeble test methods that appear in the literature have each been the subject of only a single paper and have not become widely accepted, therefore the documentation is limited, and the test results have not yet been correlated to the behavior of actual restrained weldments.

Selection of the Controlled Heating Rate Test (CHRT)

Of the test methods that were reviewed, the most thoroughly documented and eco-

KEYWORDS

Strain-Age Cracking
Superalloys
CHRT Test
Weldability
Weldability Test
Nickel-Based Alloys

M. D. ROWE is with Dept. of Civil Environmental Engineering, Michigan Technological University, Houghton, Mich.

nomical method appears to be the controlled heating rate tensile test (CHRT) developed in the late 1960s (Ref. 1). In the CHRT, a solution annealed tension-test specimen is heated at a controlled rate to a test temperature in the γ' precipitation temperature range, then pulled to failure. The test is repeated at various temperatures over the γ' precipitation temperature range, and the minimum elongation for a given alloy is taken as an indicator of susceptibility to strain-age cracking. The test is as economical as a standard tensile test and can be performed on the same equipment.

The CHRT differs from some other test methods in that it does not employ a holding time in the γ' precipitation temperature range. The continuous heating rate of the CHRT is selected to simulate the heating rate that would occur in post-weld solution annealing of a fabricated component in a batch furnace. In typical fabrication practice, the welded component is heated as rapidly as possible through the γ' precipitation temperature range to the solution annealing temperature; thus the use of holding times in the precipitation temperature range would not be relevant to fabrication practice.

Fawley et al. evaluated several different mechanical tests and found that the CHRT gave the best correlation to the results of highly controlled and automated restrained-circular-patch tests (Ref. 1). The CHRT was conducted on mill-annealed material that was not subjected to welding or to a HAZ thermal cycle. Subjecting the specimen to a weld thermal cycle reduced the measured CHRT ductility, but did not alter the ranking of the various heats of Rene 41 alloy, thus it was determined that cracking susceptibility was a property of the base metal, and that the HAZ thermal cycle was not a necessary component of the test.

Fawley et al. went on to evaluate the effects of heat treatment and test atmosphere on cracking susceptibility using the CHRT. Testing in an inert atmosphere or vacuum was found to significantly improve resistance to cracking. The most important parameter determining the resistance of various Rene 41 alloy heats to cracking was found to be grain size. Fawley et al. found that heats of Rene 41 alloy that exhibited greater than 3.5% elongation in the CHRT did not crack in the circular patch test. The effectiveness of controlling grain size and of heat treatment in an inert atmosphere to avoid strain-age cracking was later confirmed in production at Rocketdyne.

The CHRT was selected for this investigation based on its simplicity and the reported successful use of this test to quantitatively rank the effectiveness of various processing methods and material variables in preventing strain-age cracking of Rene 41 alloy fabrications.

Materials

Standard mill production material was used for testing in the form of 0.063-in.-(1.6-mm-) thick sheet. Alloys and heat numbers are listed in Table 1. Material was tested in the mill-annealed condition, the condition in which it would be purchased and welded by fabricators. Grain size and hardness of the as-received material prior to testing are given in Table 2. Standard mill processing of Waspaloy and R-41 alloys involved a final anneal in air, followed by water-spray quench. Standard processing of 718, X-750, and 263 alloys involved a final bright anneal in a hydrogen atmosphere, followed by cooling in hydrogen, which results in a slower cooling rate than spray quench. The processing details for PK33 alloy were not provided. All specimens were removed in an orientation transverse to the rolling direction of the sheet.

Controlled Heating Rate Test (CHRT) Procedure

The CHRT procedure (Ref. 1) was adapted for use on a standard tensile test frame with a resistance-heated clamshell-type furnace. The sheet tensile specimen had a reduced section measuring 0.063 in. thick by 0.5 in. wide by 2.25 in. long ($1.6 \times 12.7 \times 57$ mm). Gage marks were placed on the specimen, and then it was loaded into the test frame. Specimens had a tendency to break in gage marks placed on the reduced section, so elongation was measured based on gage marks made in the shoulders of the test specimen and percent elongation was calculated based on the adjusted length of the reduced section, as described in ASTM Specification E21-92. Three thermocouples were wired to the test specimen, at the top, middle, and bottom of the reduced section.

Table 1 — Chemical Composition of Alloys, wt-%

Alloy	Waspaloy	Waspaloy	R-41	R-41	R-41	263	X-750	718	718	PK33
Heat	2590-9-6512	2590-9-6519	2490-9-8303	2490-1-8322	2490-1-8326	2990-0-9524	2750-9-7619	2180-2-9831	2180-0-9991	ZNJ2879
Al	1.39	1.45	1.48	1.53	1.53	0.49	0.68	0.61	0.53	1.89
B	0.007	0.008	0.008	0.006	0.003	0.002	—	0.005	0.004	0.003
C	0.08	0.08	0.09	0.09	0.09	0.06	0.04	0.05	0.06	0.048
Nb	0.07	0.05	<0.05	<0.05	<0.05	<0.05	0.94	5.02	5.15	—
Co	12.76	13.33	10.92	10.86	10.47	19.62	<0.05	0.31	0.23	13.10
Cr	18.68	19.07	19.12	19.43	19.18	20.49	15.3	18.18	18.47	18.82
Fe	0.80	1.03	3.63	3.64	3.50	0.41	8.32	18.13	18.53	0.68
Mo	4.25	4.3	9.66	10.09	10.14	5.85	<0.05	3.02	3.07	7.22
Ni	58.28	57.6	51.84	50.89	51.9	50.9	71.51	52.7	52.59	56.0
Si	<0.05	0.05	0.09	0.03	0.04	0.06	0.22	0.11	0.14	0.22
Ti	2.89	2.92	3.12	3.22	3.14	2.16	2.42	1.02	0.99	1.90
Zr	0.04	0.04	0.01	0.01	0.01	0.01	—	—	—	0.014
Al+Ti+ Nb+Ta (at.-%)	6.44	6.54	6.92	7.17	7.06	3.65	4.88	5.70	5.55	6.28
Fraction γ' at 500°C[a]	0.27	0.27	0.29	0.30	0.30	0.15	0.19	0.23	0.22	0.27
DUCT[b]	3.347	3.646	3.283	3.609	2.558	1.192	–2.376	1.066	0.558	–1.247

Notes: (a) The equilibrium molar fraction γ' at 500°C was calculated using Pandat software. For Alloy 718, the fractions γ' and γ'' were added together.
(b) DUCT = 25.3%C – 15.4%Si + 299%B

It was necessary to test without the use of an extensometer in order to reduce the thermal mass sufficiently to achieve the desired heating rate. The specimen was heated to 1100 ±3°F (593 ± 1.7°C) in the clamshell furnace and held at that temperature for 10 min. The three temperature zone controls on the furnace were then increased to achieve a uniform heating rate of 25° to 30°F/ min. until the desired test temperature was reached. Upon reaching the temperature, the three controllers were set to hold that temperature during the test, and the specimen was pulled to failure at a constant crosshead speed of 0.063 in./min (1.6 mm/min). The specimen was removed, cooled, and the elongation was measured from the failed specimen. The yield stress in the CHRT was calculated from a 0.2% offset on a load-displacement curve.

Other Tensile Test Methods

In addition to the CHRT, three other tensile-test methods were used for comparison. The ASTM E21 tensile test involves maintaining the test temperature for 20 min prior to testing, maintaining a strain rate of 0.005/min to the yield point, then increasing the crosshead speed to 0.11 in./min to fracture. Two variations on the ASTM test were also used, in which the specimen was held at the test temperature for 5 or 20 min, and the specimen was pulled to failure at a constant crosshead speed of 0.063 in./min.

Calculation of Phase Fraction Diagrams

Thermodynamic phase balance calculations were conducted using *Pandat*™ software (v. 5.0), made by CompuTherm LLC, along with the Ni-Data (v. 6) database of thermodynamic properties, made by Thermotech Ltd.

Results and Discussion

CHRT Results

The CHRT results for the set of commercial alloys are given in Table 2 and plotted in Fig. 1. Each value in Table 2 represents the average of duplicate tests. The average difference between duplicate values of the CHRT minimum elongation was 0.5 percentage points for the data set in Table 2. Three heats of R-41 alloy were tested, and these gave the lowest elongation values in the test program at 2 to 3%. Two heats of Waspaloy alloy were tested, giving the next-lowest elongation values at about 3.5%. PK33 alloy performed similarly to Waspaloy. The two heats of 718 alloy performed similarly to each other, but differed from the other alloys. Alloy 718 exhibited a ductility minimum of 7 to 8% near 1450°F (788°C), then recovered to more than 50% elongation at 1500°F (816°C). Alloys with a high fraction of γ' exhibited low ductility over a greater temperature range than 718 alloy and those with a smaller fraction of γ', including 263 and X-750 alloys. Alloy 718 is known to be relatively weldable compared to other precipitation-hardenable alloys, but is not immune to cracking during heat

Table 2 — Controlled Heating Rate Test (CHRT) Results

Alloy	Heat	Grain Size (ASTM)	Hardness (RB)	Test Temp (°F)	Test Temp (°C)	AGL Elongation (%)	0.2% Yield Strength (ksi)	Ultimate Strength (ksi)
Waspaloy	2590-9-6512	4–4.5	93.7	1400	760	8.1	62.2	84.2
Waspaloy	2590-9-6512	4–4.5	93.7	1450	788	5.0	67.3	81.4
Waspaloy	2590-9-6512	4–4.5	93.7	1500	816	3.4	69.1	80.7
Waspaloy	2590-9-6512	4–4.5	93.7	1600	871	4.8	63.6	73.0
Waspaloy	2590-9-6519	4–4.5	93.7	1450	788	4.2	71.7	86.4
Waspaloy	2590-9-6519	4–4.5	93.7	1500	816	3.5	74.6	87.5
Waspaloy	2590-9-6519	4–4.5	93.7	1550	843	3.6	71.9	82.2
R-41	2490-9-8303	5–5.5	97.9	1400	760	6.3	85.2	108.1
R-41	2490-0-8303	5–5.5	97.9	1500	816	2.8	93.9	104.3
R-41	2490-9-8303	5–5.5	97.9	1550	843	2.4	85.0	95.4
R-41	2490-9-8303	5–5.5	97.9	1600	871	5.1	78.1	87.7
R-41	2490-1-8322	6	25.9[a]	1450	788	4.6	95.5	113.0
R-41	2490-1-8322	6	25.9[a]	1500	816	3.1	92.3	104.5
R-41	2490-1-8322	6	25.9[a]	1550	843	3.3	85.7	94.2
R-41	2490-1-8322	6	25.9[a]	1600	871	21.4	74.4	85.1
R-41	2490-1-8326	5.5–6	27.4[a]	1450	788	3.7	96.5	114.8
R-41	2490-1-8326	5.5–6	27.4[a]	1500	816	2.2	93.5	106.0
R-41	2490-1-8326	5.5–6	27.4[a]	1550	843	2.5	84.3	94.8
R-41	2490-1-8326	5.5–6	27.4[a]	1600	871	36.0	78.5	85.0
263	2990-0-9524	3.5	88.8	1400	760	19.0	46.0	79.7
263	2990-0-9524	3.5	88.8	1450	788	19.0	45.7	76.5
263	2990-0-9524	3.5	88.8	1500	816	22.9	52.0	69.8
263	2990-0-9524	3.5	88.8	1550	843	31.7	47.7	56.7
X-750	2750-9-7619	5.5–6	90.2	1400	760	11.8	61.7	71.8
X-750	2750-9-7619	5.5–6	90.2	1450	788	11.6	57.0	64.7
X-750	2750-9-7619	5.5–6	90.2	1500	816	13.0	56.3	59.9
X-750	2750-9-7619	5.5–6	90.2	1550	843	19.4	43.5	46.0
718	2180-2-9831	6.5–7	96.3	1400	760	9.2	82.9	96.5
718	2180-2-9831	6.5–7	96.3	1450	788	7.1	76.7	90.0
718	2180-2-9831	6.5–7	96.3	1500	816	39.4	69.6	77.6
718	2180-2-9831	6.5–7	96.3	1550	843	53.6	56.7	61.2
718	2180-0-9991	8	96.0	1400	760	9.9	81.5	96.9
718	2180-0-9991	8	96.0	1450	787	8.3	82.2	90.8
718	2180-0-9991	8	96.0	1500	816	38.7	75.5	79.5
PK33	ZNJ2879	4.5	99.2	1500	816	3.6	63.6	81.5
PK33	ZNJ2879	4.5	99.2	1550	843	3.8	68.7	79.5
PK33	ZNJ2879	4.5	99.2	1600	871	5.4	65.4	72.3

(a) Rockwell C scale.

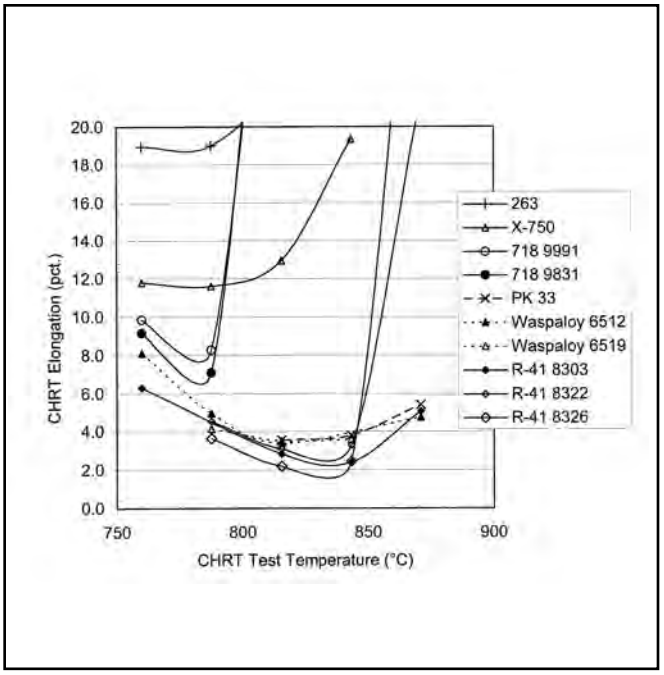

Fig. 1 — Controlled heating rate test (CHRT) elongation vs. test temperature for several commercial, wrought superalloys. Each symbol represents the average of duplicate tests.

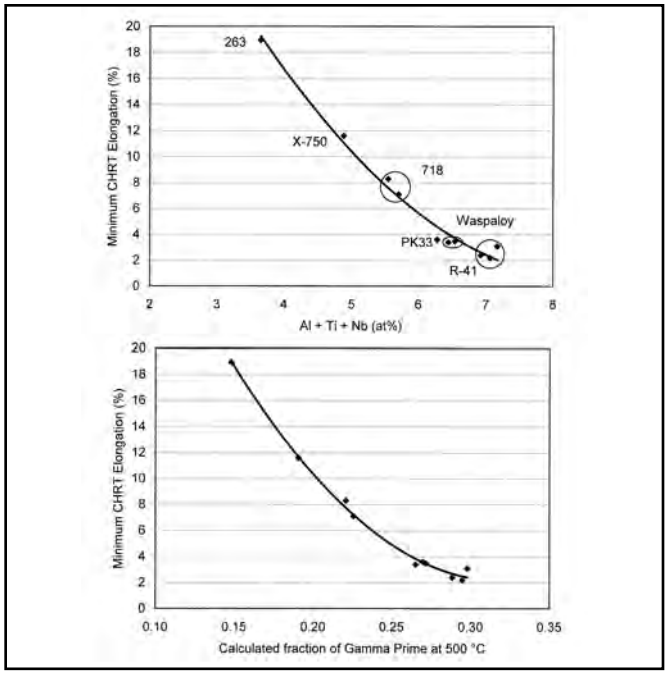

Fig. 2 — Correlation of CHRT elongation to total γ′-forming alloy content (top) and to calculated fraction of γ′ (bottom) for commercial, wrought superalloys. Each symbol represents the average of duplicate tests.

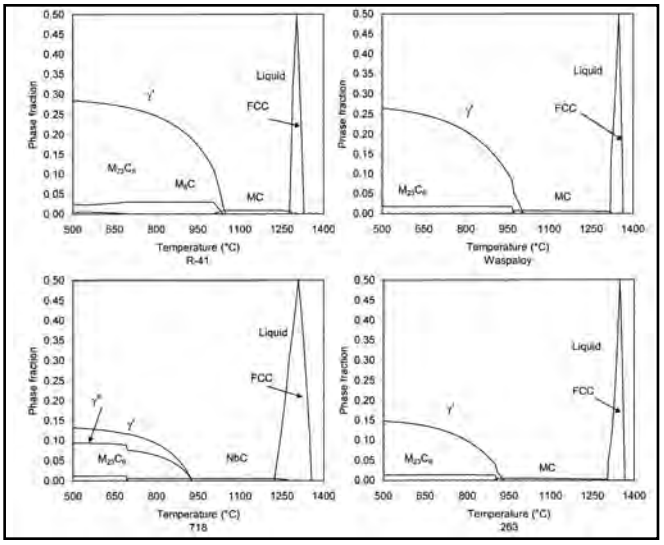

Fig. 3 — Calculated phase fraction diagrams for four alloys. Intermetallic phases were suspended in the calculations to represent the phase mixture that may form in a short-term test, such as the CHRT.

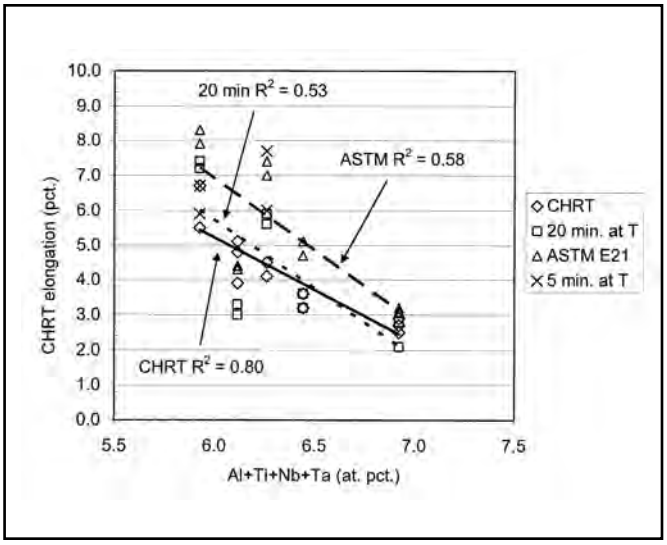

Fig. 4 — Comparison of the ranking given to a set of five alloys by the controlled heating rate tensile test (CHRT) to the ranking given by other tension test methods. Each symbol represents a single test result. All alloys were tested at 1500°F (816°C). Low R^2 values for the 20-min and ASTM test methods indicate the lack of a continuous trend for these two test methods, in contrast to the CHRT results.

treatment. Alloys X-750 and 263 gave greater elongation values than the other alloys, 12% and 19% respectively, owing to their lower fraction of γ′.

Correlation of CHRT Results to Chemical Composition and Calculated Phase Fractions

Minimum elongation values for the alloys correlated well to the total atomic percentage of γ′-forming elements. The minimum CHRT elongation also correlated well to the fraction of γ′ in each alloy at 500°C, as shown in Fig. 2. Calculated fractions of γ′ are given in Table 1. The equilibrium fraction of γ′ was calculated at the relatively low temperature of 500°C to represent the maximum fraction of γ′ that each alloy is capable of forming. The total atomic percentage of γ′-forming elements is considered to be a surrogate for the maximum fraction of γ′ that is capable of forming in each alloy. At the test temperature where the CHRT minimum elongation occurred, the equilibrium fraction of γ′ is less than the fraction at 500°C, and the actual fraction present in the alloy during the test would depend on the kinetics of precipitation, dissolution, and coarsening in each alloy. Calculation of the

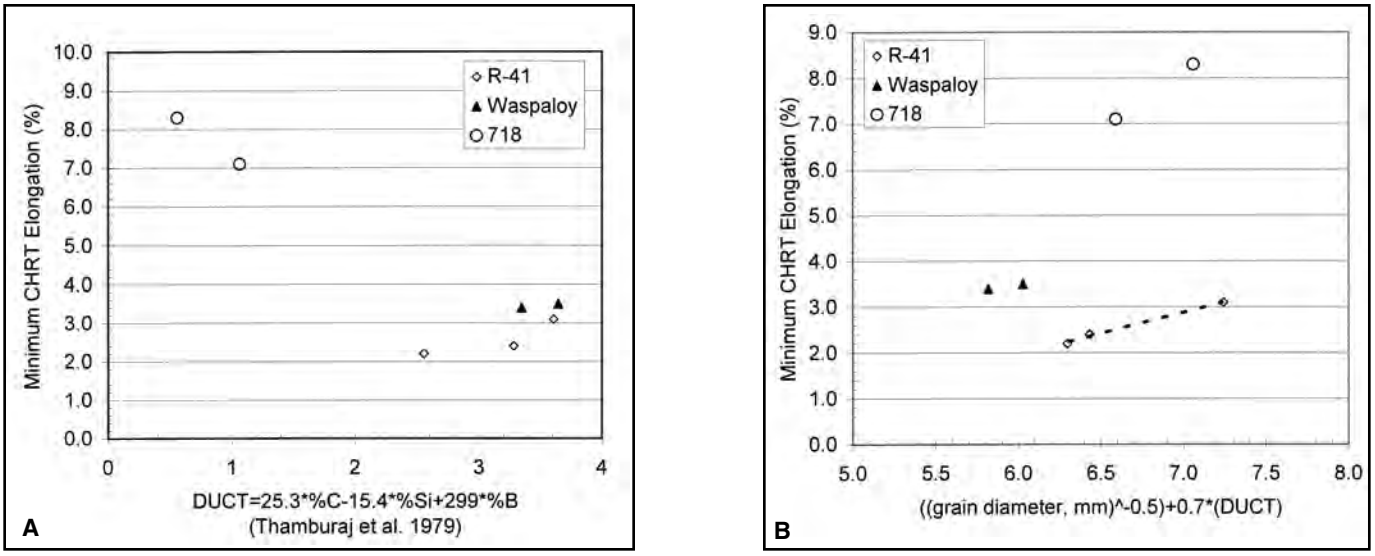

Fig. 5 — A — Correlation of CHRT elongation to the empirical parameter DUCT developed by Thumberaj et al.; B — correlation of CHRT elongation to a function of inverse square root of grain diameter and DUCT scaled by a factor of 0.7.

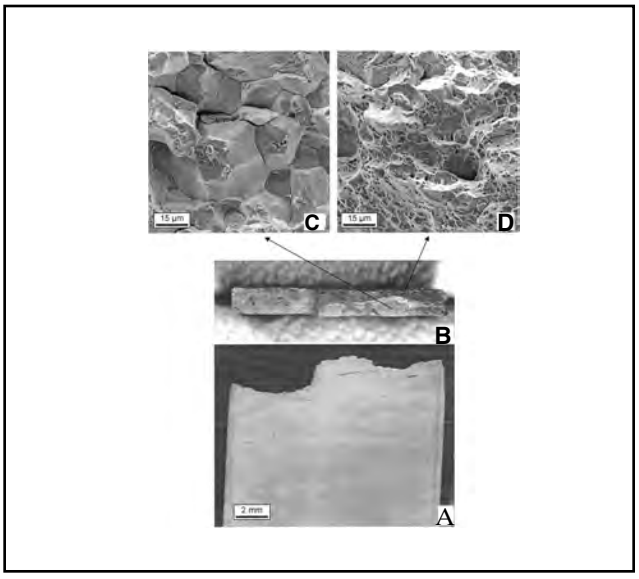

Fig. 6 — Fracture surface of a R-41 alloy CHRT specimen tested at the minimum ductility temperature. Light optical images of the test specimen showing intergranular cracking. A and B — Brittle intergranular and ductile rupture regions on the fracture surface. Secondary electron images. C — intergranular fracture region; D — ductile region.

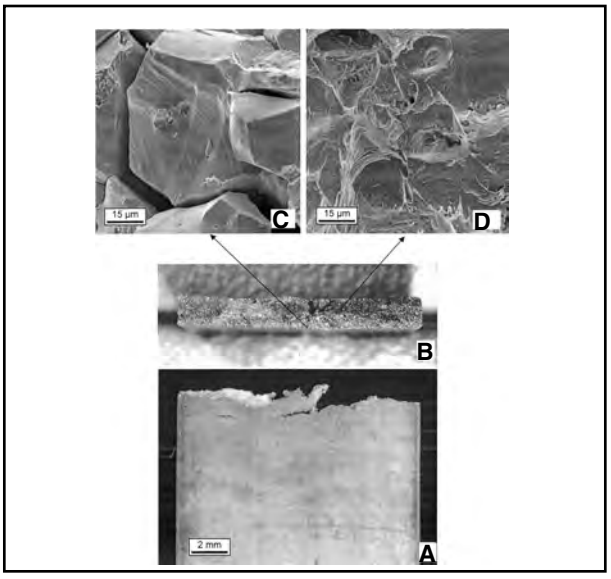

Fig. 7 — Fracture surface of a Waspaloy alloy CHRT specimen tested at the minimum ductility temperature. Light optical images of the test specimen showing intergranular cracking. A and B — Brittle intergranular and ductile rupture regions on the fracture surface. Secondary electron images; C — intergranular fracture region; D — ductile region.

γ fraction at 500°C resulted in a better correlation with CHRT minimum elongation than when the fraction of γ was calculated at the test temperature, suggesting that a large supersaturation, or thermodynamic driving force, for precipitation of γ during the heating phase of the test is an important contributor to cracking susceptibility. The calculated equilibrium fraction of γ at the test temperature is not as representative of the condition of the alloy during the test because the material spends a relatively short time at the test temperature and the precipitation strengthening has already occurred at a lower temperature during the heating stage of the test.

Calculated phase fraction diagrams for four representative alloys are shown in Fig. 3. Intermetallic phases that were predicted to form but are known to have slow kinetics, such as η in 263 alloy, δ in 718 alloy, σ and μ in Waspaloy and R-41 alloys, were suspended from the calculations in order to represent the phase mixture that is likely to form from the solution-annealed alloys during a short-term test. Both γ and γ″ are known to coexist in 718 alloy, but the experimentally measured ratio of γ″ to γ fraction is greater than what is predicted in Fig. 3 (Ref. 12). It was necessary to add the two phase fractions together for 718 alloy to conform to the trend in Fig. 2. While γ″ is thought to form after a relatively long time, it is clear that 718 alloy strengthened substantially during the time scale of the CHRT procedure, as evidenced by the 77 to 83 ksi yield strength shown in Table 2 for the 1400° and 1450°F test temperatures. It is not certain whether the

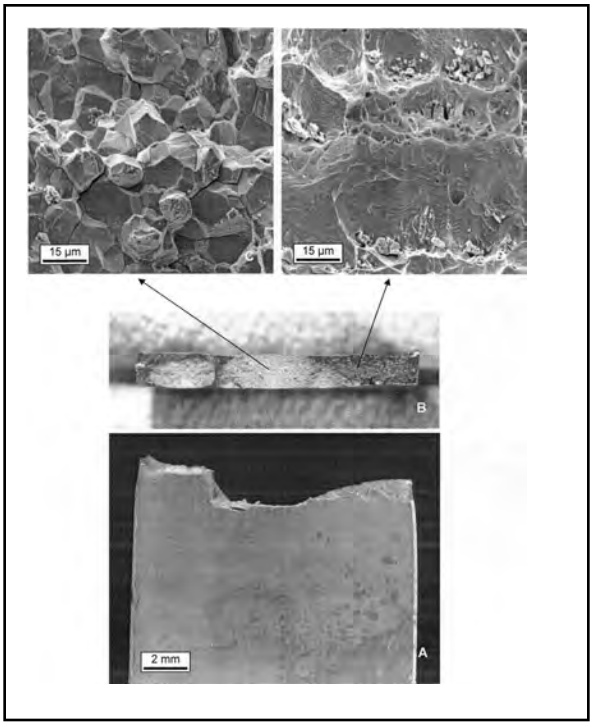

Fig. 8 — Fracture surface of a 718 alloy CHRT specimen tested at the minimum ductility temperature. Light optical images of the test specimen showing intergranular cracking. A and B — Brittle intergranular and ductile rupture regions on the fracture surface. Secondary electron images; C — intergranular fracture region; D — ductile region.

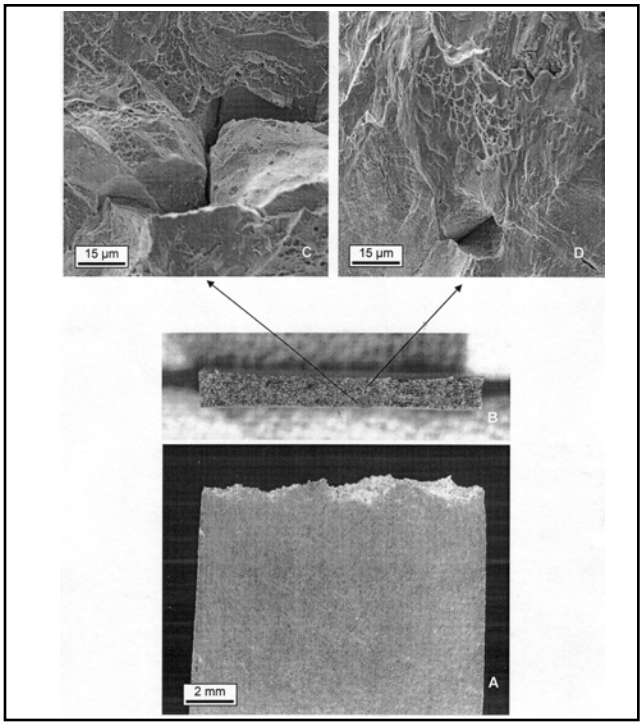

Fig. 9 — Fracture surface of a 263 alloy CHRT specimen tested at the minimum ductility temperature. A and B — Light optical images of the test specimen showing the fracture surface. Secondary electron images; C — Mixed ductile rupture; D — intergranular mode of fracture.

strengthening is caused by precipitation of γ, γ', or both in the CHRT procedure.

The CHRT gave elongation values of 2 to 3% at 1500°F (816°C), while three tensile tests of R-41 alloy (heat 2490-9-8303) in the fully aged condition [1400°F (760°C) 8 h] gave 8, 11, and 18% elongation at 1500°F. The alloy exhibited significantly greater ductility in the aged condition than in the CHRT, even though the yield strength was slightly higher in the aged condition. Metallography revealed that the alloy developed grain boundary carbides after the standard-aging treatment, which were not present after the CHRT. Grain boundary precipitates that form during the standard aging treatment may strengthen the grain boundaries and increase resistance to intergranular cracking. These precipitates do not have time to form during the CHRT, even though the alloy has sufficient time to develop most of its strength, which may contribute to the very low ductility exhibited in the CHRT. A similar phenomenon may be expected to occur during heat treatment of material fabricated in the solution-annealed condition. Alternatively, the low ductility displayed by R-41 alloy in the CHRT has been attributed to precipitation of hyperfine γ on heating, which may coarsen during the standard aging treatment (Ref. 1).

Comparison of CHRT to Other Tensile Test Methods

The CHRT results are compared to results of other tensile test methods for a set of five alloys with varying levels of γ-forming elements in Fig. 4. The results in Fig. 4 are from five different alloys; the content of γ-forming elements is not the only compositional variable. Each symbol represents a single test result. Two or three replicates are plotted for each condition so that the reproducibility of the test methods can be seen. All alloys were tested at 1500°F (816°C), which is very close to the minimum ductility temperature for each alloy. It is expected that, in general, the susceptibility to strain-age cracking increases as the content of γ-forming elements increases in the alloy. Linear regression lines are used in Fig. 4, not to suggest a theoretical basis for a linear trend, but simply to illustrate that the CHRT data show a decreasing trend in CHRT elongation as a function of increasing content of γ-forming elements, while the other tensile test methods do not show a continuous trend. The CHRT results gave a better correlation ($R^2 = 0.80$) with the total content of γ-forming elements in the alloy than the other two test methods ($R^2 = 0.53$ and 0.58), as indicated in Fig. 4.

The result of holding at the test temperature for 20 min was to increase ductility for some alloys and decrease ductility for other alloys in comparison to the CHRT, in which the test was conducted immediately upon reaching the test temperature. Holding at the test temperature for 5 min produced variable results and was not pursued further. There is no trend line for the 5-min-at-temperature test in Fig. 4 because of limited data. Comparison of CHRT results to 20-min-at-temperature results in Fig. 4 reveals that ductility decreases with holding time for some alloys while increasing or remaining constant for others. The effect of holding times in the precipitation temperature range was not pursued further because holding times are not relevant to actual fabrication practice.

The results of the ASTM test were similar to the 20-min-at-temperature test, but with increased ductility as a result of the higher strain rate. Strain rate has been shown to have a significant effect on the measured ductility of Waspaloy alloy (Ref. 9). Sensitivity to strain rate is consistent with a mechanism of environmental embrittlement by oxygen. The CHRT offers the advantage of simulating the microstructure that would occur in a fabrication during the initial heating cycle to the solution-annealing temperature, while the other tensile test methods, which involve longer holding

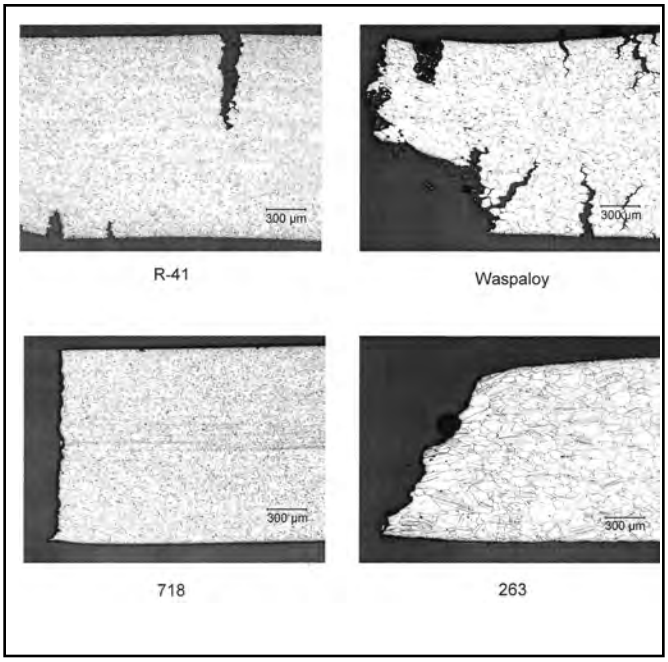

Fig. 10 — Cross sections of the fracture surfaces of CHRT test specimens tested near the minimum ductility temperature.

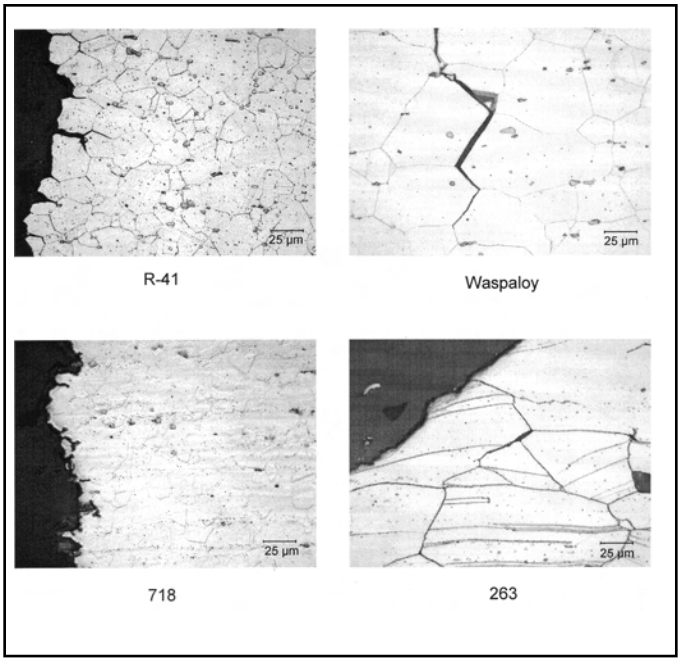

Fig. 11 — Microstructures near the fracture surface of CHRT specimens tested near the minimum ductility temperature.

times, do not simulate the process of post-weld heat treatment. Furthermore, the relatively slow strain rate used in the CHRT more closely simulates the slow buildup of strain in a restrained fabrication than would a faster strain rate.

Comparison of CHRT Results to a Predictor of Strain-Age Cracking Resistance

Thumberaj et al. (Ref. 13) investigated the influence of chemical composition on strain age cracking of Rene-41 alloy. Using the heat compositions and CHRT results reported by Fawley et al. (Ref. 1) and some others, they correlated the CHRT results to chemical composition using regression analysis. An empirical parameter called DUCT was developed, which predicted susceptibility of R-41 alloy heats to strain-age cracking. Higher values of DUCT indicated greater ductility and greater resistance to cracking. The empirical relationship indicated a beneficial influence of carbon and boron, and a detrimental influence of silicon on CHRT results.

Values of DUCT were calculated for each of the alloys tested in the present program, and are given in Table 1. For each of the alloys having data for multiple heats, the CHRT elongation is plotted as a function of DUCT in Fig. 5A. The DUCT parameter successfully predicted the better-performing heats for R-41 and Waspaloy alloys, but not for 718 alloy. The valid correlation for R-41 and Waspaloy alloys suggests that carbon and boron have a beneficial influence and silicon has a detrimental influence on CHRT behavior in both alloys. Boron is known to improve resistance to intergranular cracking and carbon may strengthen grain boundaries through carbide precipitation, or it may limit grain growth by carbide pinning of grain boundaries. The DUCT parameter was developed by regression analysis on heats of R-41 alloy only, so it follows that it would predict the performance of a similar alloy such as Waspaloy, but not effectively predict the performance of a very different alloy such as 718. Furthermore, DUCT does not take into account the influence of variations in γ'-forming elements because these were held relatively constant in the heats of R-41 alloy from which DUCT was developed, whereas the minor elements, carbon, boron, and silicon, varied in these heats to a greater extent.

Fawley et al. commented that high silicon promotes grain growth, but did not explain the mechanism for this phenomenon (Ref. 1). Fawley et al. plotted the minimum CHRT elongation as a function of the inverse square root of grain diameter and found a linear relationship (Ref. 1). The strong trend suggested that grain size is the main source of heat-to-heat variations in Rene 41 alloy, and that compositional variations are important in sofar as they influence grain size. In the present investigation, the best-performing heats of 718 alloy and R-41 alloy had a slightly finer grain size than the other heats, as indicated in Table 2. In Fig. 5B, the CHRT ductility is plotted against a function of both grain diameter and the DUCT chemical composition parameter, producing a favorable correlation for all three alloys. While the present data set is too small to develop a reliable empirical relationship, the results indicate that both grain size and chemical composition are important variables in determining strain-age cracking behavior.

Fractography and Metallography

Strain-age cracking failures typically exhibit an intergranular fracture surface (Refs. 1, 2). Fractography was carried out on the CHRT specimens to determine if the test simulated this intergranular cracking phenomenon. A set of four alloys, including R-41, Waspaloy, 718, and 263, was selected to illustrate the range of fractographic behavior exhibited among the alloys tested. Details of the fracture surfaces are shown in Figs. 6–9. The alloys that exhibited relatively low ductility, R-41 (Fig. 6), Waspaloy (Fig. 7), and 718 (Fig. 8), exhibited regions of brittle, intergranular fracture that initiated from the surface and propagated into the center of the specimen. This was especially visible in the case of 718 alloy (Fig. 8). Somewhat different behavior was exhibited by 263 alloy in that intergranular fracture did not appear to initiate from the surface. Alloy 263 exhibited the greatest resistance to cracking of the alloys tested. Fracture occurred by a mixture of ductile rupture and intergranular separation throughout the thickness of the specimen.

Cross sections of the fractured specimens are shown in Fig. 10. Intergranular cracks that initiated from the surface are clearly visible in R-41 and Waspaloy alloys.

In the case of 718, the entire specimen thickness separated by brittle-intergranular fracture at the location of the cross section shown in Fig. 10, although there were also areas of ductile rupture, as shown in Fig. 8. The fracture of 263 alloy was ductile with single grain facets that separated by intergranular cracking scattered throughout the thickness. Microstructures near the fracture surface are shown in Fig. 11. Locations of intergranular cracking are shown for R-41, Waspaloy, and 718 alloy. In the case of 263 alloy, the ductile fracture surface is shown with a few internal intergranular separations that did not propagate into cracks.

The presence of intergranular cracking suggests that the phenomenon of strain-age cracking had successfully been reproduced in the CHRT. Strain-age cracking is known to propagate intergranularly. The initiation of cracking at the surface of the specimens suggests environmental embrittlement by oxygen (Refs. 1, 4, 14). While embrittlement by oxygen appears to contribute to a further reduction in ductility, it was noted that heat treatment in vacuum improves ductility but does not entirely eliminate cracking in Rene 41 alloy (Ref. 14).

Summary

Ranked according to the CHRT minimum elongation, the susceptibility of wrought superalloys to strain-age cracking is as follows from greatest to least: R-41, Waspaloy, PK-33, 718, X-750, and 263. Alloy 718 exhibited low ductility over a lesser temperature range than the other alloys, which is not taken into account in ranking the alloys simply by minimum ductility. The CHRT minimum ductility correlated well with the sum of Al+Ti+Nb on an at.-% basis and with the calculated fraction of γ' at 500°C. The CHRT provided an effective and economical means of ranking alloys, and gave a ranking that was consistent with expectations based on the literature.

Acknowledgments

Rupinder Sharma and Lee Pike of Haynes International are gratefully acknowledged. Sharma operated the controlled heating rate tensile test apparatus and Pike provided technical input and assisted with *Pandat* calculations.

References

1. Fawley, R. W., Prager, M., Carlton, J. B., and Sines, G. 1970. Recent studies of cracking during postwelding heat treatment of nickel-base alloys. *WRC Bulletin* No. 150. Welding Research Council, NY.

2. Lepkowski, W. J., Monroe, R. E., and Rieppel, P. J. 1960. Studies on repair welding age-hardenable nickel-based alloys. *Welding Journal* 39(9): 392-s to 400-s.

3. Weiss, S., Hughes, W. P., and Macke, H. J. 1962. Welding evaluation of high temperature sheet materials by restrained patch testing. *Welding Journal* 41(1): 17-s to 22-s.

4. Thompson, E. G., Nunez, S., and Prager, M. 1968. Practical solutions to strain-age cracking of Rene 41. *Welding Journal* 47(7): 299-s to 313-s.

5. Hughes, W. P., and Berry, T. F. 1967. A study of the strain-age cracking characteristics of welded Rene 41 — Phase I. *Welding Journal* 46(8): 361-s to 370-s.

6. Wu, K. C., and Herfert, R. E. 1967. Microstructural studies of Rene 41 simulated weld heat-affected zones. *Welding Journal* 46(1): 32-s to 38-s.

7. Dix, A. W., and Savage, W. F. 1971. Factors influencing strain-age cracking in Inconel X-750. *Welding Journal* 50(6): 247-s to 252-s.

8. Franklin, J. E., and Savage, W. F. 1974. Stress relaxation and strain-age cracking in Rene-41 weldments. *Welding Journal* 53(9): 380-s to 387-s.

9. Nakao, Y. 1988. Study on reheat cracking of Ni-based superalloy. Waspalloy. *Transactions of the Japan Welding Society,* 19(1): 66–74.

10. Lin, W. 2000. A methodology for quantifying postweld heat treatment cracking susceptibility. Abstracts of papers, 81st Annual AWS Convention, p. 158.

11. Norton, S., and Lippold, J. C. 2001. Development of a Gleeble-based test for postweld heat treatment cracking susceptibility. Abstracts of papers, 82nd Annual AWS Convention, p. 129–130.

12. Chaturvedi, M. C., and Han, Y. 1983. Strengthening mechanisms in Inconel 718 superalloy. *Metal Science* 17(3): 145–149.

13. Thamburaj, R., Goldak, J. A., and Wallace, W. 1979. The influence of chemical composition on post-weld heat treatment cracking in Rene-41. *SAMPE Quarterly*, (7): p. 6–12.

14. D'Anessa, A. T., and Owens, J. S. 1973. Effects of furnace atmosphere on heat treat cracking of Rene 41 weldments. *Welding Journal* 52(12): 568-s to 575-s.

Papers are Sought for American Welding Society's 2006 Professional Program

MIAMI - December 22, 2005 - The American Welding Society's Technical Papers Committee has issued a call for papers for the Professional Program at the 2006 FABTECH International & AWS Welding Show, scheduled for October 31-November 2 at the Georgia World Congress Center in Atlanta, Georgia.

The Professional Program will include presentations on topics of interest to welding practitioners and managers, researchers, and advanced students. Papers are sought in three categories:

- Technical/Research Oriented, involving new science or engineering relevant to welding, joining, and allied processes.
- Applied Technology, involving new or unique applications of known principles of joining science or engineering.
- Welding Education, involving successful education and training methods at all levels that are relevant to the welding industry.

Papers may be process-oriented or materials-oriented, and may include modeling of welding processes. Preference will be given to papers with a clearly communicated benefit to the welding industry.

Abstracts may be submitted using the form enclosed in this issue of the *Welding Journal* at the end of the Research Supplement or the online form located at *www.aws.org/w/s/survey/standard.html?survey_start=abstractsubmittal*.

For more information, contact Gladys Santana, AWS manager of conferences and seminars, at (800/305)443-9353, ext. 223, or via email at *gladys@aws.org* .